Photo-Kinetic Study of Irgacure 784 Dye in an Epoxy Resin Photopolymer

Article *in* Proceedings of SPIE - The International Society for Optical Engineering · May 2009

DOI: 10.1117/12.820839

CITATIONS
3

READS
728

4 authors:

Dusan Sabol

22 PUBLICATIONS **234** CITATIONS

SEE PROFILE

Michael R. Gleeson

Eblana photonics

108 PUBLICATIONS **1,698** CITATIONS

SEE PROFILE

Shui Liu

University College Dublin

25 PUBLICATIONS **673** CITATIONS

SEE PROFILE

John T Sheridan

University College Dublin

496 PUBLICATIONS **7,566** CITATIONS

SEE PROFILE

Photo-Kinetic Study of Irgacure 784 Dye in an Epoxy Resin Photopolymer

Dušan Sabol, Michael R. Gleeson, Shui Liu and John T. Sheridan*

UCD School of Electrical, Electronic and Mechanical Engineering,
UCD Optoelectronic Research Centre,
SFI Strategic Research Cluster in Solar Energy Conversion,
College of Engineering, Mathematical and Physical Sciences,
University College Dublin, Belfield, Dublin 4,
Republic of Ireland.

ABSTRACT

Photopolymers are promising as holographic recording media as they are inexpensive, versatile materials, which can be made sensitive to a broad range of wavelengths. A deeper understanding of the processes, which occur during holographic grating formation in photopolymers, is necessary in order to develop a fully comprehensive model, which represents their behaviour. One of these processes is photo-initiation, whereby a photon is absorbed by a photosensitiser producing free radicals, which can initiate free radical polymerisation. These free radicals can also participate in polymer chain termination (primary termination) and it is therefore necessary to understand their generation in order to predict the temporally varying kinetic effects present during holographic grating formation. In this paper, a study of the photoinitiation mechanisms of Irgacure 784 dye, in an epoxy resin matrix, is carried out. This is achieved by analysing the temporal evolution of a series of simultaneously captured experimental transmittance curves, captured at different wavelengths, but at the same location, to enable the change in photon absorption during exposure to be estimated. We report on the experimental results and present a theoretical model to predict the physically observed behaviour.

Keywords: Photopolymer, Photoinitiation, Photoinitiator, Holography, Irgacure 784, Photosensitiser, Dye

1. INTRODUCTION

In the literature, extensive research is currently being carried out on a variety of photopolymer materials. Their low cost, selfprocessing capability and low loss make them promising materials for various applications. In order to reach their full material potential, accurate material models, based on reproducible experimental data sets, will be necessary. In particular such models are needed to identify and permit optimization of crucial operational parameters.

In this paper we focus on the photo-initiation stage, which takes place during exposure. This stage begins with photon absorption by a photosensitiser typically leading to its dissociation and free radicals generation. The resulting free radicals can react with: (i) monomer, initiating growth of polymer chains and therefore refractive index changes, (ii) an inhibitor, thus being scavenged, and (iii) monomer radicals thus terminating an active polymer tip.

Photosensitiser consumption reduces the absorbance of a photopolymer layer. Thus the number of free radicals produced can be estimated by measuring the resulting variation in the material transmission curve. In this paper we

* Corresponding Author: **e-mail:** john.sheridan@ucd.ie **Tel:** +353-1-716-1927; **Fax:** +353-1-283-0921

Holography: Advances and Modern Trends, edited by Miroslav Miler, Miroslav Hrabovský,
Proc. of SPIE Vol. 7358, 735804 · © 2009 SPIE · CCC code: 0277-786X/09/$18 · doi: 10.1117/12.820839

study the case of a dye where photo-cleaving generates chemical products, which can absorb at the exposing green wavelength. This additional absorption during exposure can lead to an inaccurate estimate of the rate of production of free radicals, therefore photon absorption by the effect of photoinitiation inactive (non-initiating) species must be understood. In order to separate the effects of multi-component absorption we used a red probe laser beam, which does not affect the photoinitiator dissociation but is attenuated by the absorptive intermediate product. A decrease of the probe beam output intensity then provides information about the absorption by the intermediate product at the recording green wavelength and we can thus extract absorption information about both the inactive product, and the photoinitiator from the measured absorptions.

1.1 Material composition

Our photopolymer material consists of two very different polymerizable systems. The first system is made of a combination of low refractive index epoxy resin matrix and amine hardener. These spontaneously crosslink with each other and form a rigid mesh structure (matrix), which accommodates the other components in a mechanically stable way. The second system is a mixture of high refractive index vinyl monomers, which react via free radical photo-polymerization, to form polymer chains in the exposed regions. The free radicals are generated in the bright regions by dissociation of the photoinitiator. Before exposure the matrix crosslinking takes place exclusively between the epoxy resin and the amine hardener with little chemical interaction with the rest of the chemicals present, i.e. the vinyl monomers and photoinitiator. This type of material design permits the recording of high refractive index modulations in mechanically stable layers, which can be cast to large thicknesses.

1.2 Proposed rate equations; flow chart

Our interest is to be able to predict the material response. As noted behaviour has been observed that suggests the production of a new absorber, which affects the photo-kinetic processes present during recording. We want to identify the new absorber and quantify its' effects based on results in the literature and our experimental observations. To do so we make several assumptions regarding the interactions and the chemical reactions which take place and the corresponding rates appearing in the rate equations derived, see Section 3.3. A flowchart is present in Section 3.1 which describes the processes i.e. compounds (participants) and their relationship during photoinitiation.

1.3 Set of experiments is proposed

The experimental transmittance data, changes during exposure because the photopolymer transmittance variations are not only driven by photosensitiser removal but because of the generation of the new absorber. One recorded transmission curve is therefore not sufficient to determine the photoinitiator consumption. Therefore another laser, whose light is not absorbed by the photosensitiser, but whose intensity is attenuated by the new absorber, is used to provide a second transmittance curve.

2. MATERIAL COMPOSITION

Our study was carried out on modified photopolymer composition, which was first proposed by Trentler *et al.*[1,2]. This photopolymer is made of three essential parts:

1. *Thermally cured matrix*, which acts as a stable binder. It is made of an epoxy resin and an amine hardener which crosslink with each other at ambient temperature. They are selected to have high transparency, low refractive indices and minimal chemical interaction with the other compounds. We used Poly(propylene glycol) Diglycidyl ether (n = 1.464) and Diethylenetriamine (n = 1.484).
2. *Photopolymerizable monomer mixture* with high refractive index which produces refractive index variation depending on the exposing light pattern. It consisted of 1-Vinyl-2-pyrrolidone (n = 1.51) and 9-Vinylcarbazole (n = 1.68).
3. *Photosensitiser,* Irgacure 784 dye, which initiates photo-polymerization.

This basic composition may be extended by introducing other chemicals, for example; terminators, chain transfer agents, reducing agents etc. The composition used and constituent details are shown in Table 1.

Function	Compound	Acronym	Mass [g]
MATRIX	Poly(propylene glycol) diglycidyl ether	PGE	10
	Diethylenetriamine	DTA	2.19
WRITING MONOMERS	1-Vinyl-2-pyrrolidone	NVP	0.9125
	9-Vinylcarbazole	NVC	0.9125
PHOTOSENSITISER	Irgacure 784	Dye	0.614
INHIBITOR	2 6-Di-tert-butyl-4-methylphenol	BHT	0.0068

Table 1: Material composition.

The material (dry layer) preparation procedure is as follows:

1. The required weights of each component are placed into 100 ml beaker. The photosensitiser is added last and following its inclusion, every step is performed under a red light conditions.
2. The mixture is heated and gently stirred at 50°C for approximately 20 minutes.
3. The composition is cooled down and placed into the bell jar and vacuum pumped for approximately 1.5 hours to remove air and other gas.
4. Material is then sucked into a syringe while the viscosity is still low. It is necessary to wait until it has optimal consistency. Viscosity must be high enough to prevent the free flow of the material over the glass substrate. On the other hand it must be low enough to adhere to the glass and allow air bubbles to emerge from the layer.
5. On the microscope glass slide, plastic spacers of a desired thickness are positioned. Then an appropriate volume of material with suitable viscosity is drop cast. Then the material is carefully covered by a second glass slide to avoid trapping air bubbles. A weight is placed on the top to ensure the uniform spread of material before hardening.
6. Samples are laid out to cure at least 6 hours. They are stored in the dark at room temperature.

3. PHOTOINITIATION

As stated the photopolymer contains the photosensitiser dye Irgacure 784, the chemical structure of which is shown in Figure 1 (a). Its schematic representation is shown in Figure 1 (b) where **Cp** stands for η^5-cyclopentadien-1-yl and **R** stands for aryl. It is a titanocene compound, which does not require an electron donor in order to produce free radicals. After the absorption of light quanta to which Irgacure 784 is sensitive, the molecule undergoes homolytic cleavage of the aryl-metal bond, giving an aryl radical[3] and a metal compound in a low oxidation state. This new metal compound can still absorb light. If such absorption does take place at 532 nm, it will not contribute to the free radical production but it will reduce the number of photons which when absorbed lead to photoinitiation. Experimentally we observe a smaller quantity of light passing through the photopolymer layer. However, if we assume there is just a single absorber present, it would appear that there is a higher photoinitiator concentration present.

If an attempt is made to relate the value of transmittance to the free radical production[2] we will overestimate number of free radicals created. Consequently, this material composition requires a new approach compared to that previously used for dyes such as Methylene Blue and Erythrosin B[4,5]. This new approach must take into account absorptive inactive photoproducts in order to accurately predict quantitative photoinitiator absorption and free radical generation.

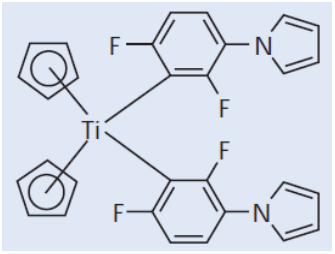

(a)

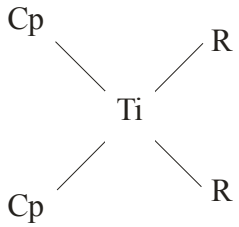

(b)

Figure 1: Irgacure 784 dye: (a) Chemical structure[6] and (b) schematic structure of Cp_2TiR_2.

In the next section our assumptions regarding the photochemical processes and reactions, which take place during and after exposure are discussed and a flowchart is presented to illustrate these interactions. Then, in Section 3.2, we proceed to describe our experimental setup.

3.1 Photochemical processes

The decomposition during illumination of several different titanocene photoinitiator systems, including Irgacure 784, has been studied in the literature and several possible reaction paths have been proposed[7-13]. In our study we assume that photoinitiation proceeds as follows: A photon interacts with Irgacure 784 molecule bringing it to an active state Eqn (1), which can then continue to dissociate.

$$Cp_2TiR_2 + h\upsilon \longrightarrow Cp_2TiR_2^{*}. \tag{1}$$

The activated molecule can return to the ground state by reaction with a quencher Z, either by emitting a photon, Eqn (2a), or through molecular collision, Eqn (2b).

$$Cp_2TiR_2^{*} + Z \longrightarrow Cp_2TiR_2 + h\upsilon, \tag{2a}$$

$$Cp_2TiR_2^{*} + Z \longrightarrow Cp_2TiR_2. \tag{2b}$$

The quencher becomes inert after the reaction with the activated photoinitiator and does not participate in any further reactions. Thus successful photocleavage splits Irgacure 784 into two reactive species, as illustrated in Figure 2.

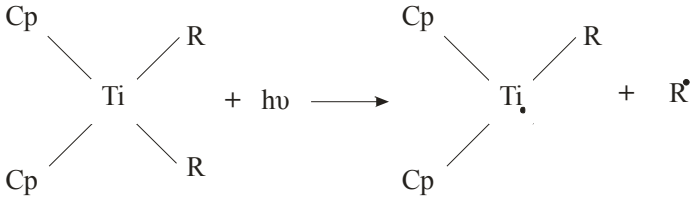

Figure 2: Photocleavage of Irgacure 784.

We assume that the titanium centered molecule produced exhibits a modified broad absorption spectrum which includes both the green exposing and the red probing wavelengths. This absorptive intermediate state eventually reacts to form a stable transparent state. In Figure 3 we assign a capital letter to each component. These letters are used later to represent chemical concentrations in the model presented in Section 3.3, i.e. they are used to represent molar concentrations of particular species. A schematic reaction path is presented in Figure 3.

Irgacure 784……A

↓

Absorptive Intermediate Product……B

↓

Final Transparent Product……C

Figure 3: Proposed reaction path, or cascade of photochemical reactions.

The mechanisms governing the transitions between the $A \rightarrow B \rightarrow C$ states are summarized in the flowchart in Figure 4.

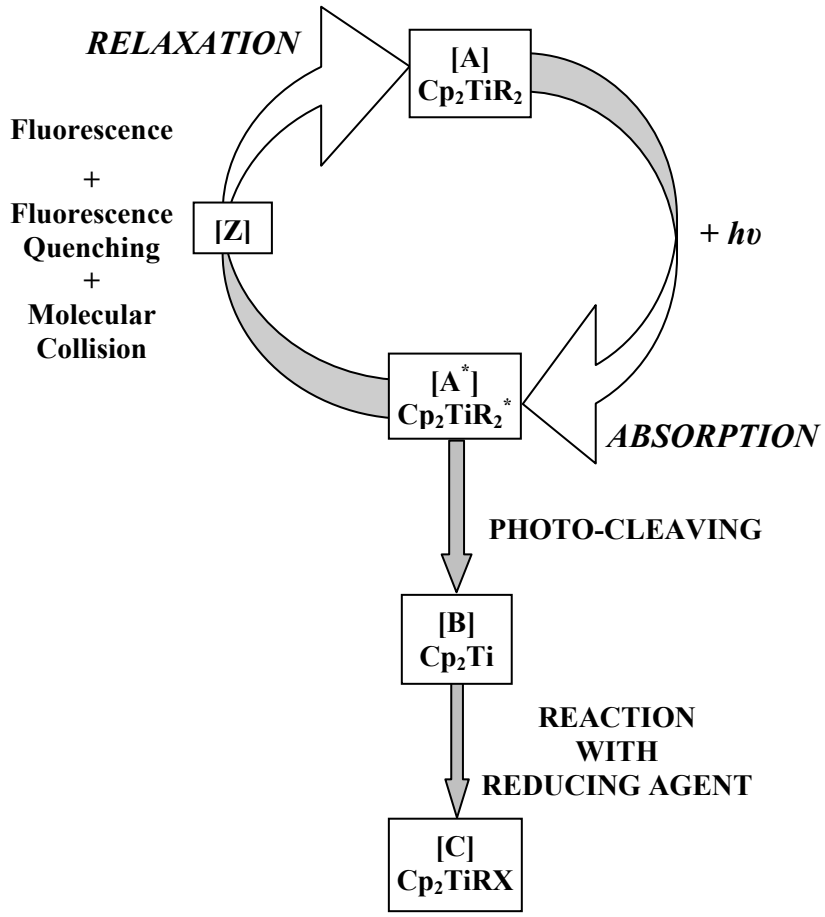

Figure 4: Photochemical flowchart.

In this section we have discussed the properties of the photoinitiator and reactions through which it is removed during the process of photoinitiation. All the chemical products and processes are illustrated in the flowchart in Figure 4. In the next section experiments are described which we have performed in order to measure the required the green exposing and red probing transmittance data.

3.2 Experimental method

As noted in the previous section, the cleavage of the Irgacure 784 produces free radicals and metal products in low oxidation state with amended absorptive properties. A second probe laser with a wavelength outside the sensitive region of the photosensitiser, but which is absorbed by the metal compound, is introduced to illuminate the exposed layer. In Figure 5 the absorption spectrum of Irgacure 784 is shown. Since very little absorption appears to take place at wavelengths greater than 550 nm a probe He-Ne laser wavelength 633 nm was used.

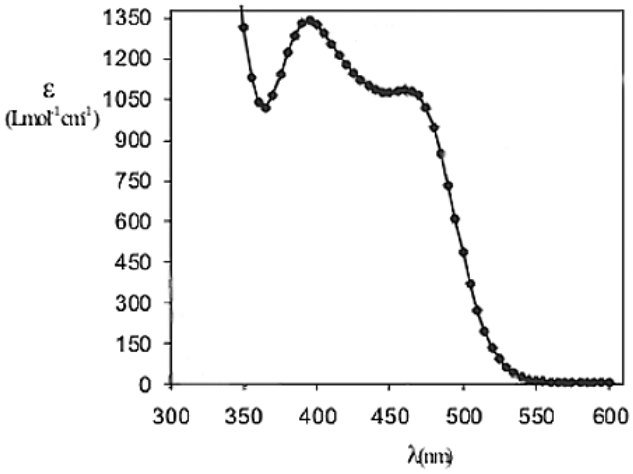

Figure 5: Absorption spectrum of Irgacure 784[7].

Before exposing the layer using the green laser the photopolymer was first probed with the 633 nm laser beam (operating at a wavelength outside of the absorption band of Irgacure 784) to verify its insensitivity at that wavelength. The transmitted probe power stayed constant as expected. The layer was then illuminated with the 532 nm beam from a diode-pumped solid state laser. Probing the exposed region using the red beam it was found that there was a reduction in the red transmitted probing power as exposing in the green continued.

One possible explanation might be that loss took place due to material scatter. We exclude this option because there was no observable decrease in optical quality of the bleached layer, at the shorter 532 nm exposure wavelength the scatter is likely to be stronger than at 633 nm but no loss is observed in the green exposing transmission curve. The final transmittance value at both wavelengths was 90 %, which approaches the maximum possible after allowing for losses due to Fresnel reflections. For completeness we note that an initial dip in the amount of light transmitted was previously reported[14] however this was followed by growth of the transmission curve. Another possible explanation of observed experimental results is the generation of new compounds, which absorb at 633 nm and also at 532 nm. In what follows we assume another absorber is generating which causes this change in the red probe beam transmission curve.

All these measurements were performed using the experimental setup shown in Figure 6.

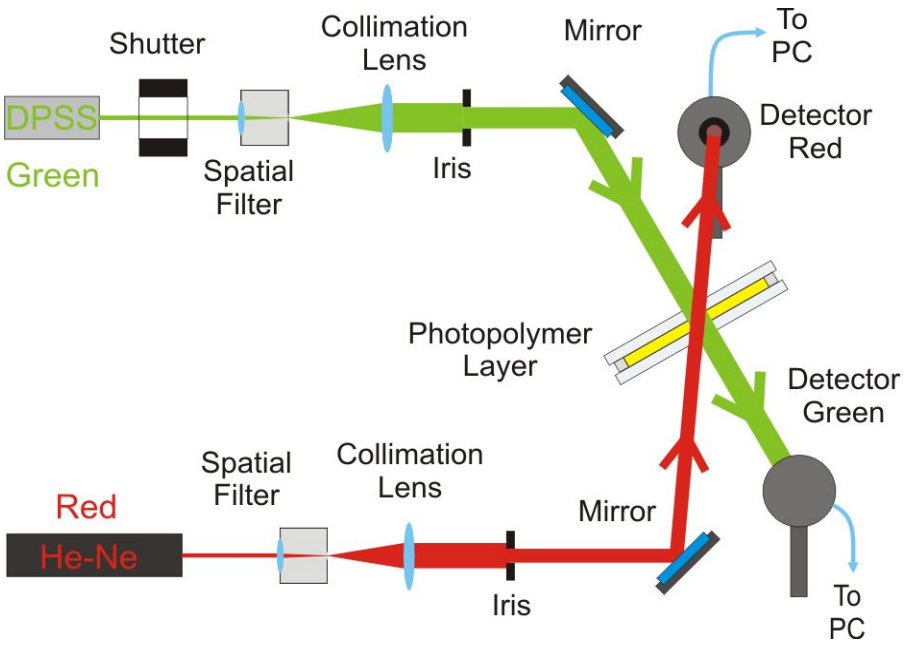

Figure 6: The experimental setup to measure transmittance curves of the green (exposing) and red (probe) beam.

Two spatially filtered and collimated laser beams, at wavelengths 532 nm and 633 nm, expose and probe the photopolymer layer respectively. The iris diameter of the green beam, 0.56 cm, this is chosen to give an exposed area of 0.25 cm^2. The red aperture iris size is chosen to be slightly smaller. The photopolymer layer is placed into the exposing green beam and the transmitted power is recorded. The exact exposure time is determined using the electronic shutter. The red probing beam simultaneously passes through the same exposed area at an angle to the green beam. The red probe beam is always present independent of the green beam.

Having described the experimental setup we now proceed to develop a set of differential equations governing the time evolution of the absorbers concentrations. These concentration values can then be used to describe both the red and the green transmission curves presented in the next section.

3.3 Physical model

We begin by assuming that time variations of the transmission intensity are due to the changes of the absorber concentrations, which are both uniformly spatially distributed in the photopolymer layer. At time $t = 0$ s the only absorber is the photoinitiator dye, the initial concentration of which we know from the material composition. During exposure by the green light, the photoinitiator concentration decreases and a new absorber is generated. The normalized transmission of the exposing and the probing light beams is then governed by the following equations[14]:

Transmission of the green (532 nm) exposing light:

$$\frac{I_{Out}^{G}(t)}{I_{0}^{G}} = T_{532}(t) = \exp\left[-\left(\varepsilon_{A}A(t) + \varepsilon_{B@532}B(t)\right)d\right], \tag{3}$$

Transmission of the red (633 nm) probe light:

$$\frac{I_{Out}^{R}(t)}{I_{0}^{R}} = T_{633}(t) = \exp\left[-\varepsilon_{B@633}B(t)d\right]. \tag{4}$$

where $A(t)$ and $B(t)$ are the concentrations of photoinitiator and the new absorber respectively, ε_A, $\varepsilon_{B@532}$ and $\varepsilon_{B@633}$ are the molar (wavelength appropriate) absorptions of the photoinitiator A and the new absorber B, and d is the layer thickness. Both $T_{532}(t)$ and $T_{633}(t)$ are corrected for Fresnel reflections.

The photoinitiator is transparent at 633 nm hence its molar absorption at this wavelength is equal to zero. Thus there is no $A(t)$ term in the transmittance equation for 633 nm, Eqn (4). The transmission curves are governed by the concentration changes of $A(t)$ and $B(t)$, while ε_A, $\varepsilon_{B@532}$ and $\varepsilon_{B@633}$ remain constants. The changes in the absorber concentrations are modeled by the following differential equations (5.1-5.5):

$$\frac{dA(t)}{dt} = -\frac{\phi_A}{d} I_0^G \left\{1 - \exp[-\varepsilon_A A(t) d]\right\} + k_z A^*(t) Z(t) . \tag{5.1}$$

This rate equation, Eqn (5.1), which governs the variation of the photoinitiator concentration describes its removal from a ground state $A(t)$ [mol/cm^3] to the activated state $A^*(t)$ [mol/cm^3], and its recovery or relaxation back to the ground state because of the photoinitiator absorption or regeneration respectively. Φ_A [mol/Einstein)] represents a number of molecules removed due to the absorption of the green light, I_0^G [Einstein/cm^2] is the exposing green intensity, $\varepsilon_A A(t)$, with units [cm^{-1}] is the photoinitiator absorbance and d [cm] is the layer thickness. The second term in Eqn (5.1) models the regeneration from the activated state [mol/cm^3] state through a reaction with a quencher $Z(t)$ [mol/cm^3] to the ground state at rate k_z [cm^{3}mol^{-1}s^{-1}]. The initial concentrations are $A(t = 0\text{ s}) = 1.04$ mol/cm^3 and $A^*(t = 0\text{ s}) = 0$ mol/cm^3.

The quencher concentration $Z(t)$ [mol/cm^3] is used up during the reaction with the photoinitiator in the activated state and thus loses its ability to bring the activated molecule to the ground state. The quencher concentration decrease is governed by Eqn (5.2) which starts from an initial concentration value of $Z(t = 0\text{ s}) = Z_0$ mol/cm^3

$$\frac{dZ(t)}{dt} = -k_z A^*(t) Z(t) . \tag{5.2}$$

Eqn (5.3) describes the production and the removal of the concentration of the photoinitiator in the activated state $A^*(t)$ [mol/cm^3], with negative signs appearing in this equation in front of the terms which previously appeared on the right side of Eqn (5.1). Another negative removing term is included which depends on the concentration of the activated state $A^*(t)$ acting with rate k_B [s^{-1}]

$$\frac{dA^*(t)}{dt} = \frac{\phi_A}{d} I_0 \left(1 - \exp[-\varepsilon_A A(t) d]\right) - k_z A^*(t) Z(t) - k_B A^*(t) . \tag{5.3}$$

The removal term $k_B A^*(t)$ appearing in Eqn (5.3) is also present in Eqn (5.4) as a generating term of the B product, with B product being removed with rate $k_C B(t)$,

$$\frac{dB(t)}{dt} = k_B A^*(t) - k_C B(t) . \tag{5.4}$$

The B product is then converted into the C product (transparent state) governed by Equation (5.5),

$$\frac{dC(t)}{dt} = k_C B(t) . \tag{5.5}$$

We use this set of first-order coupled differential equations to model the kinetic behavior, and proceed to apply this model to fit experimental transmittance data in the next section.

3.4 Experimental Results and the Estimated Parameter Values

Experiments were repeatedly performed, using the standard material composition (Section 2), and using the experimental procedure and setup described in Section 3.2. Three different green exposing intensities were used until in each case saturation was reached.

Numerical fitting was achieved by varying physical parameters manually. In all cases attempts were made to achieve good visual fits, to both the green and the red transmittance data points, with the smallest spread of parameter values. The resulting green and red transmission curve fits are plotted in Figure 7, Figure 8 and Figure 9 for intensities values i.e. 1, 4 and 16 mW/cm^2. In all the figures the two transmittances, (red, green), are plotted as functions of the exposing time in seconds.

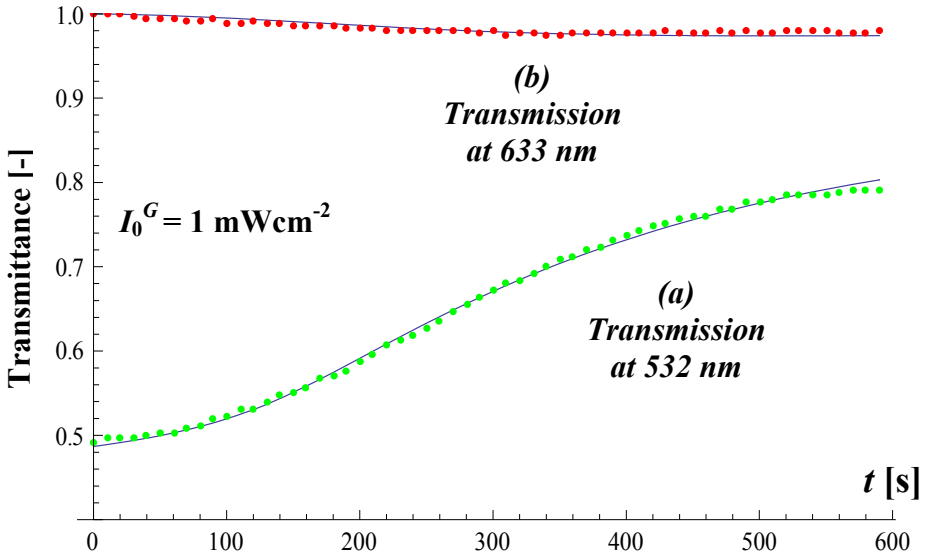

Figure 7: experimental data, solid lines fits to, (a) green exposing, and (b) red probing transmittance data. Intensity of the green beam 1 mW/cm^2.

The extracted parameters are listed in Table 2 for three different green exposure intensities, I_0^G [mW/cm^2]. Other parameters are: i) Z_0 [mol cm^{-3}] the initial quencher concentration which returns activated photoinitiator into the ground state, k_z [cm^{3}mol^{-1}s^{-1}] is the rate with which this reaction occurs, ii) k_B and k_C [s^{-1}] the rate constants determining the rates of production of the B and the C product respectively, iii) Φ_A [mol/Einstein] the quantum efficiency which quantifies the number of removed initial state molecules per absorbed photon, iv) $\varepsilon_{B@633}$ and $\varepsilon_{B@532}$ [cm^2/mol] are the molar absorption values estimated for the B product at 532 and 633 nm respectively.

The initial green transmission value depends upon the photoinitiator initial concentration, the sample thickness and its optical quality. The initial slope and induction band duration depend on the initial concentration of the quencher Z_0, the rate k_z with which it reacts with the activated photoinitiator and the quantum yield Φ_A. These parameters also affect the initial part of the red transmission curve. The quantum yield and the rates of production of B and C products determine the slope of the middle part of both the red and the green transmission curves. The saturation parts of both transmission curves depend on the molar absorptions of the B product and the rates of its generation and removal.

I_0^G [mW/cm^2] (Figure)	Z_0 [mol cm^{-3}] ($\times 10^{-5}$)	k_z [cm^{3}mol^{-1}s^{-1}] ($\times 10^5$)	k_B [s^{-1}]	k_C [s^{-1}] ($\times 10^{-3}$)	Φ_A [mol/ Einstein]	$\varepsilon_{B@633}$ [cm^2/mol]	$\varepsilon_{B@532}$ [cm^2/mol]	RMSE [-] Green ($\times 10^{-4}$)	RMSE [-] Red ($\times 10^{-4}$)
1 (Fig. 7)	4	1	1	1	10.5	7,500	30,000	5.6	4.5
4 (Fig. 8)	4	1	1	1	5.1	11,000	34,000	11	5.7
16 (Fig. 9)	4	1	1	1	4.8	11,000	36,000	31	17

Table 2: Parameters extracted by fitting both the red and the green transmission curves simultaneously.

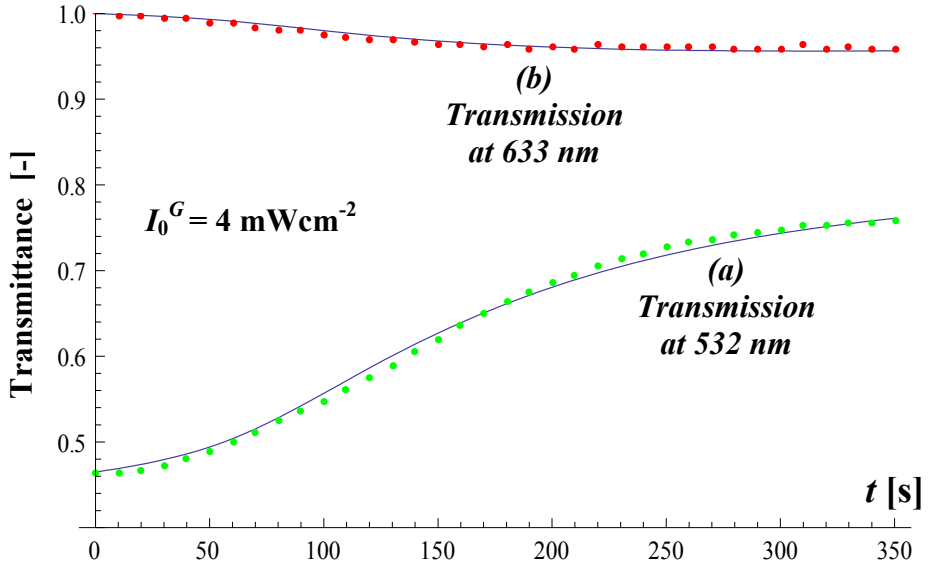

Figure 8 experimental data, solid lines fits to, (a) green exposing, and (b) red probing transmittance data. Intensity of the green beam 4 mW/cm^2.

We began this fitting process by examining the lowest intensity case, i.e. 1 mW/cm^2 shown in Figure 7. In the 4 mW/cm^2 case in Figure 8 we found that it was possible to retain the same values for Z_0, k_z, k_B, k_C from the previous case and find the values for quantum efficiency and molar absorption values of the *B* product. The resulting fit is shown in Figure 8. In order to produce a satisfactory fit or the 16 mW/cm^2 case, Figure 9, it was found to be only necessary to vary the quantum yield and the molar absorption values of the *B* product. The quality of the fit is quantified using the Root Mean Square Error (RMSE). This quantifies the deviation of the fit from the experimental data and is calculated for both transmission curves using Eqn (6),

$$\mathrm{RMSE} = \frac{1}{N}\sqrt{\sum_{i=1}^{N}\left(T_{Fit} - T_{Data}\right)^2}\ , \qquad (6)$$

where T_{Fit} is the value predicted by model at a particular time, T_{Data} is the corresponding measured value and N is the number of samples used over the time intervals shown.

In all cases, (for each exposing intensity), the same sampling rate is used, i.e. one sample every 10 s until saturation was reached. Therefore graphs corresponding to experiments for longer exposure times contain more samples. The values of RMSE were found to increase with increasing exposing intensity. Therefore the model seems to more accurately predict results for weaker exposures. Further increases of the exposing intensity cause an initial dip in the transmission curve[13] which are not predicted to exist using the current model. This behaviour and the significant differences in the estimated values of the molar absorption for different exposing intensities indicate that in the system there appears to be another absorber at 532 nm the presence of which has yet to be accounted for. Extending the model so that it more accurately represents the physical situation are the goals of our future work.

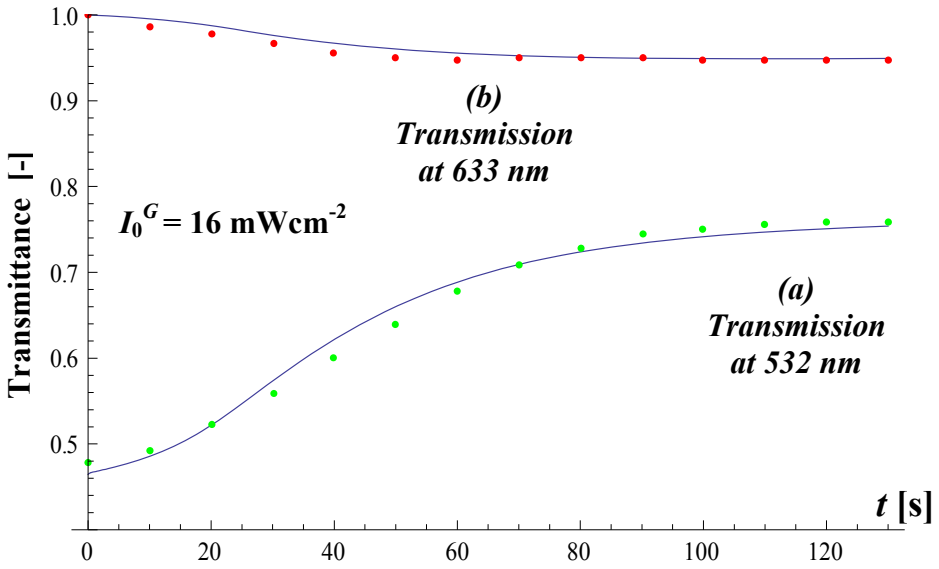

Figure 9: Dots experimental data, solid lines fits to, (a) green exposing, and (b) red probing transmittance data. Intensity of the green beam 16 mW/cm^2.

4. CONCLUSIONS, DISCUSSION OF THE RESULTS, AND FUTURE WORK

In this paper we describe an initial investigation of the consumption of photoinitiator, Irgacure 784, in a photopolymer layer composed of an epoxy matrix with vinyl monomers. We have proposed and demonstrated that at least one new broadband absorber is produced during photoinitiation. Rate equations have been proposed to describe the photo-chemical reactions. The equations were solved for three different exposure intensities in order to obtain the best fit to measured transmittance curves for a layer. These are then used to extract as consistent a set of physical parameters values as possible by manually fitting the transmittance data. Reasonable rate values for use in the rate equations were obtained, however the estimated molar absorptions (at both wavelengths) of the new absorber (B product) show high variations for different intensities. Measurements to find molar absorption are difficult to perform. We are able to measure an *absorbance* which is the molar absorption multiplied by the absorber's concentration but we do not know the exact concentration of the new absorber (B product) and the transparent C product. High quantum efficiencies $\Phi_A > 1$, suggest the existence of another, dark removal mechanism which, even after weak short exposures, is capable of fully using up whole photoinitiator concentration. This is consistent with other research reported in the literature[15].

Therefore the variations in the estimated molar absorption of the *B* product might be due to the fact that there are other absorption(s) taking place simultaneously. For example, the reactions taking place $A \rightarrow B$ and $B \rightarrow C$ could go through an intermediate product state at some particular rate. One possibility is that the activated state A* might itself act as an absorber. If this in fact is the case then it will be possible to obtain better fits. However the resulting increase in the complexity of the model will increase the difficulty verifying such a model. One way to verify it will be if it is able to explain some specific behaviour, for example the transmission curves at higher intensities[13], (for example > 80 mW/cm^2), the observed initial dip, i.e. decrease in transmittance, and then growth to a local maximum and finally the slow bleaching. Therefore the goals for future work are: i) to improve the model further describing processes in a multi-absorbers environment in order to estimate the evolution of absorber concentrations, and ii) to better understand the photo-initiation photo-chemistry of Irgacure 784 as used in our particular photopolymer composition, thus providing a better estimation of free radical production. Once this is achieved it can be incorporated into our Non-Local Photo-Polymerization Diffusion Driven Model[16], (NPDD), to describe holographic grating formation.

5. ACKNOWLEDGMENT

We acknowledge the support of Enterprise Ireland and Science Foundation Ireland through the Research Innovation and Proof of Concept Funds and the Basic Research and Research Frontiers Programs. We would also like to thank the Irish Research Council for Science, Engineering and Technology.

6. REFERENCES

[1] T. J. Trentler, J.E. Boyd, V. L. Colvin, "Epoxy resin-photopolymer composites for volume holography," Chem. Mater., **12**, 1431-1438, (2000).

[2] M. R. Gleeson, "*Analysis of the Photochemical Kinetics in Photopolymers for Holographic Data Storage and Hybrid Photonics Circuits*," Dissertation thesis, UCD, Chapter 7, pages 237-238, (2008).

[3] J. Jakubiak, J. F. Rabek, "Photoinitiators for visible light polymerization", Polymeri, **44**, 7-8, 447-461, (1999).

[4] M. R. Gleeson, S. Liu, S. O'Duill, J. T. Sheridan, "Examination of the photoinitiation processes in photopolymer materials," Journal of Applied Physics, **104**, 0649171-0649178, (2008).

[5] S. Liu, M. R. Gleeson, J. T. Sheridan, "Analysis of the photoabsorptive behavior of two different photosensitizers in a photopolymer material," J. Opt. Soc. Am. B, **26**, 3, 528-536, (2009).

[6] http://www.ciba.com/pi.pdf .

[7] M. Degirmenci, A. Onen, Y. Yagci, S. P. Pappas, "Photoinitiation of cationic polymerization by visible light activated titanocene in the presence of onium salts," Polymer Bulletin, **46**, 6, 443-449, (2001).

[8] B. Klingert, M. Riediker, A. Roloff, "Light sensitive organometallic compounds in photopolymerization," Comments on Inorganic Chemistry, **7**, 3, 109-138, (1988).

[9] U. Zucchini, E. Albizzati, U. Giannini, "Synthesis and properties of some titanium and zirconium benzyl derivates," Journal of Organometallic Chemistry, **26**, 3, 357-372, (1971).

[10] B. Klingert, A. Roloff, "Photochemical ring slippage of bis(pentafluorophenyl)titanocene: reaction kinetics and matrix isolation of the primary photoproduct," Helvetica Chimica Acta, **71**, 8, 1858-1867, (1988).

[11] S H Lin, Y-N Hsiao, K Y Hsu, "Preparation and characterization of Irgacure 784 doped photopolymers for holographic data storage at 532 nm," J. Opt. A: Pure Appl. Opt., **11**, (2009).

[12] K. Meier, "Photopolymerization with transition metal complexes," Coordination Chemistry Review, 11, 97-110, (1991).

[13] M. W. Grabowski, K. M. Vogelhuber, D. Sabol, J. H. Chen, R. R. McLeod, J. T. Sheridan, "Absorption and bleaching dynamics of initiator in thick photopolymer exposed to Gaussian illumination," SPIE Proceeding, **7053**, 7053D-1-7053D-6, (2008).

[14] A. Dubois, M. Canva, A. Brun, F. Chaput, J.-P. Boilot, "Photostability of dye molecules trapped in solid matrices," Appl. Opt., **35**, 18, 3193-3199, (1996).

[15] N. Davidenko, O. Garcia, R. Sastre, "The efficiency of titanocene as photoinitiator in the polymerization of dental formulations," J. Biomater. Sci. Polymer Edn, **14**, 7, 733–746, (2003).

[16] M. R. Gleeson, D. Sabol, S. Liu, C. E. Close, J. V. Kelly, J. T. Sheridan "Improvement of the spatial frequency response of photopolymer materials by modifying polymer chain length," J. Opt. Soc. Am. B, **25**, 3, 396-406, (2008).